


Article

An Independent Suspension and Trafficability Analysis for an Unmanned Ground Platform

Jianying Li ^{1,*}, Yinghong Xie ²  and Yongwang Huo ²¹ School of Mechanical and Automotive Engineering, Zhaoqing University, Zhaoqing 526000, China² School of Electronic and Electrical Engineering, Zhaoqing University, Zhaoqing 526000, China

* Correspondence: lijianying@zqu.edu.cn

Abstract: The objective of this paper was to investigate and design a novel vertical- and horizontal-arm independent suspension system aimed at enhancing the autonomous obstacle-crossing capabilities of unmanned ground platforms in complex, unstructured environments such as mountainous regions, hills, and mining areas. By thoroughly considering factors such as the suspension structure design, changes in the centroid position, distribution of driving forces, and dynamic stability analysis, we proposed an innovative suspension structure. An unmanned ground platform model equipped with this suspension system was developed using ADAMS and MATLAB/Simulink. Subsequently, a joint simulation was conducted to validate the performance of the suspension system. The results indicated that the unmanned ground platform could successfully traverse vertical steps up to 370 mm high and trenches measuring up to 600 mm wide. Furthermore, when confronted with intricate obstacles including vertical barriers, trenches, and side slopes, the platform demonstrated exceptional traversing capabilities. In conclusion, the proposed suspension system significantly enhances both the obstacle-surmounting ability and the terrain adaptability of unmanned ground platforms while providing crucial technical support for their deployment in complex unstructured environments.

Keywords: unmanned ground platform; longitudinal- and transverse-arm suspension; wheeled mobile robot; MATLAB/Simulink; obstacle-surmounting ability



Academic Editors: Jie Yang and Quaxin Zhu

Received: 1 December 2024

Revised: 28 December 2024

Accepted: 11 January 2025

Published: 17 January 2025

Citation: Li, J.; Xie, Y.; Huo, Y. An Independent Suspension and Trafficability Analysis for an Unmanned Ground Platform. *Symmetry* **2025**, *17*, 128. <https://doi.org/10.3390/sym17010128>

Copyright: © 2025 by the authors. Licensee MDPI, Basel, Switzerland. This article is an open access article distributed under the terms and conditions of the Creative Commons Attribution (CC BY) license (<https://creativecommons.org/licenses/by/4.0/>).

1. Introduction

Unmanned ground platforms represent a specialized category of mobile robots. In comparison to manned ground platforms, unmanned systems can perform tasks in harsh, dangerous, harmful, and complex environments that are often inaccessible or perilous for human operators. However, during operation, direct manual intervention is not feasible; consequently, accurately evaluating and predicting obstacle performance have become challenging, which may hinder the successful execution of specific missions. Therefore, it is both urgent and essential to conduct research on the autonomous obstacle-surmounting capabilities of unmanned ground platforms in intricate terrains such as mountains, hills, and mining areas—particularly for military operations and civil emergency scenarios. The ability of an unmanned ground platform to surmount obstacles is closely linked to its mechanical structure. Shoemaker et al. emphasized that ensuring superior mobility required designing a chassis with outstanding performance characteristics—especially concerning suspension systems [1]. Erik Skultety's master's thesis [2] explored the method of unstructured terrain characterization in depth, providing theoretical support for the design of autonomous mobile robots. His research showed that in addition to advanced

sensing technology, there is a need for highly adaptable and durable mechanical designs to cope with complex environments. M. Nowakowski et al. [3] studied the removal systems of unmanned ground vehicles using modular robotic arms, demonstrating the flexibility and effectiveness of a mechanical design for specific tasks. Their finding shows that a modular and versatile mechanical design can greatly improve a UGV's mission performance.

From the perspective of adaptability to complex terrain conditions, the suspension mechanisms used by unmanned ground platforms primarily consist of active adaptive suspension and passive adaptive suspension systems. An active adaptive suspension enhances vehicle trafficability by dynamically adjusting its posture in response to terrain obstacles. However, most existing studies have predominantly focused on unmanned ground platforms navigating typical obstacles such as steps and trenches; thus, there remains a scarcity of research addressing composite obstacles. Regarding active adaptive suspensions specifically, the U.S. military's ARV-A (L) unmanned ground vehicle uses an independent articulated suspension system, where built-in drive motors and deceleration devices at the shoulder joint facilitate free rotation of the swing arm [4,5]. Additionally, He et al. [6] developed an eight-wheeled unmanned aerial vehicle (UAV) moving platform designed for enhanced operational versatility. The swing arm mechanism was integrated into a four-wheel chassis, enabling free movement through the use of hydraulic cylinders. The all-terrain unmanned vehicle developed by Zhang et al. [7], the wheel-legged compound mobile robot created by Fang et al. [8], and the platform featuring a folding waist and swing arm designed by Liu et al. [9] all use a dumpling-swing-arm suspension system. Certain rovers equipped with active suspension systems can adjust their center of mass by modifying suspension links and joints, thereby minimizing tilting when traversing a rough or sloped terrain [10,11]. This capability enhances their obstacle-surmounting performance. In contrast to active adaptive suspensions, passive adaptive suspensions do not require pre-planning of their posture; instead, they adapt to complex terrains through mechanical forces. While this approach simplifies control and reduces the driving device complexity, it limits the ability to overcome typical obstacles such as vertical barriers and trenches. Wang [12] and Zhang [13] developed all-terrain wheeled mobile robots as well as high-adaptation rescue robots based on single-longitudinal-arm independent suspensions. These designs feature wheels that are paired via active joints, allowing each joint to operate independently from others, thus ensuring that the platform maintains optimal contact with both ground surfaces and obstacles. Lindemann et al. [14] investigated the mechanical design performance of Mars rovers, highlighting that their design uses differential principles to ensure continuous wheel-ground contact while smoothing the pressure distribution between wheels and the terrain, thereby maximizing the dynamic performance potential. Wettergreen et al. [15] explored the design concept behind the Scarab probe vehicle: Scarab uses a linkage mechanism that enables its wheels to maintain effective ground contact, even on rugged landscapes. Wagner et al. [16] noted that the Nomad robot's steering suspension significantly enhanced its adaptability across various terrains. Furthermore, Apostolopoulos [17] conducted a comprehensive analysis of the Nomad robot across various dimensions and discovered that it possessed commendable lateral wheel extension capabilities to navigate complex road conditions. Additionally, several research institutions have proposed innovative passive suspension mechanisms [18–22].

In summary, in an unstructured environment, the main function of the unmanned ground platform suspension system is to ensure its adaptability to typical obstacles and compound obstacles in different terrains. Through the aforementioned literature analysis, it has been found that the suspension system of the current unmanned ground platform has the following limitations:

1. Strong vertical adaptability but insufficient horizontal adaptability: The suspension system used by many unmanned ground platforms has strong terrain adaptability and obstacle-crossing ability on the longitudinal plane. However, it often shows inadequate performance when faced with lateral challenges such as unilateral slopes, round pits, or continuous convex and convex profiles. Most existing suspensions are primarily designed for terrain adaptation in the forward direction but lack an adequate response to side tilts or obstacles. Fang et al., for example, focused on the design of mixed-wheel leg mobility.

2. Narrow range of specific applications: Some new suspension designs are only suitable for small-scale detection vehicles or are based on simplified models that do not fully take into account the actual needs of unmanned ground platforms in complex environments such as carrying heavy loads over obstacles.

To address these limitations, this study proposed a suspension system that, compared with the existing design, could solve the following problems:

1. Comprehensively solve vertical and horizontal adaptability;
2. Enhance the ability to cross obstacles;
3. Provide extensive environmental adaptability.

In this paper, using Adams View 2020 and MATLAB R2021b software tools, a model of an unmanned ground platform equipped with this advanced suspension was developed. Through joint simulations based on this model, we evaluated the performance of the independent suspension as it traversed single typical and compound obstacles to validate its effectiveness.

2. Unmanned Ground Platform Structural Design

In light of the aforementioned challenges, this paper presents a novel independent suspension structure designed to enhance the obstacle-surmounting capability and stability of unmanned ground platforms operating in complex unstructured terrains, as illustrated in Figure 1. Using both longitudinal-swing-arm mechanisms and transverse-arm mechanisms, the design ensures that when the unmanned ground platform traverses obstacles, the wheels remain closely aligned with the vertical road surface. This configuration not only optimizes tire grip, but also improves terrain adaptability without compromising the suspension's ability to lift legs and navigate over obstacles. This paper details the architecture of the new vertical- and horizontal-arm independent suspension system, which primarily comprises a vertical-swing-arm mechanism and a horizontal-arm mechanism. The system achieves adaptation to intricate terrains through connectors such as oil and gas springs. The working principle is elucidated, along with an overview of active obstacle-surmounting strategies and passive adaptation techniques.

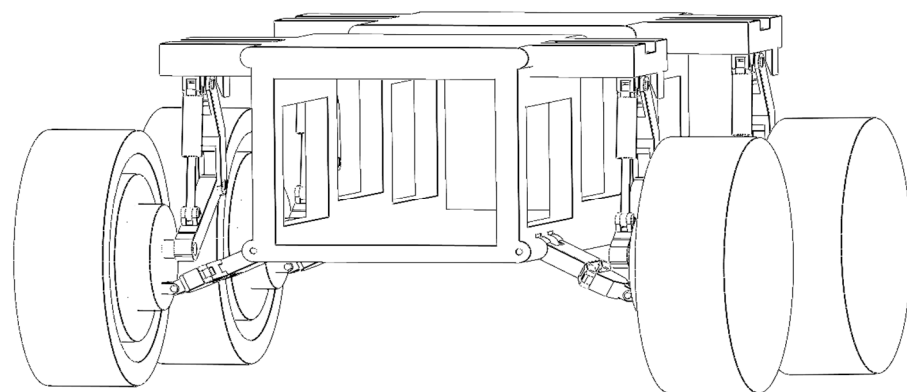


Figure 1. Structural diagram of the new vertical- and horizontal-arm independent suspension.

2.1. New Type of Independent Suspension Structure with Longitudinal and Lateral Arms

As illustrated in Figure 2, the core structure of the novel independent suspension system featuring vertical and horizontal arms proposed in this paper primarily consists of a vertical-swing-arm mechanism and a horizontal-arm mechanism. The components labeled 4–8 in Figure 2 represent the vertical-swing-arm mechanism, while those marked 9–11 correspond to the horizontal-arm mechanism. The longitudinal-swing-arm mechanism includes an adjustable longitudinal arm, which is symmetrically positioned on both sides of the vehicle body with two units. One end of each adjustable longitudinal arm, situated away from the vehicle body, is actively connected to a hydro-pneumatic spring. The opposite end of the hydro-pneumatic spring connects actively to the lower longitudinal arm. The upper side of this lower longitudinal arm is linked to an upper longitudinal arm that extends away from it. The cross-arm mechanism comprises a front cross-arm, short rods, and a rear cross-arm. The front cross-arms are symmetrically arranged on either side of the vehicle's body and are connected directly to it. Each front cross-arm is hinged at its outer end with several short rods. Meanwhile, the rear cross-arm is hinged between these short rods and one front cross-arm while extending outwardly from it toward the connection with the wheel assembly.

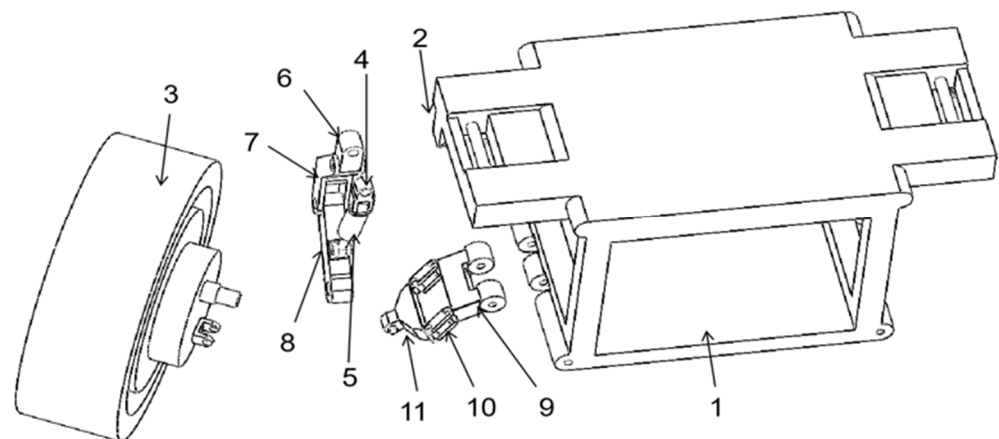


Figure 2. Schematic diagram of the decomposition structure of the new vertical- and horizontal-arm-type independent suspension: 1 is the body; 2 is the limit slot; 3 is the wheel part; 4 is the adjusting arm; 5 is the gas spring; 6 is the regulating arm; 7 is the upper arm; 8 is the lower arm; 9 is the front arm; 10 is the short rod; and 11 is the rear arm.

2.2. Working Principle

The working principle of this design is as follows. When the device is in operation, its structural design incorporates four-wheel differential steering technology, enabling it to perform in situ turning or steering on complex and narrow road terrains. This includes both the driving process and the obstacle-lifting mechanism.

In terms of the driving process, when the unmanned ground platform operates normally on a roadway, the hydro-pneumatic spring remains inactive. At this stage, it functions similarly to a conventional spring shock absorber. In unstructured environments characterized by diverse and complex terrains, such as unilateral slopes or circular depressions, the interaction between ground forces can cause a tendency toward a wheel tilt. The short arm of the mechanism can adjust passively in response to these conditions. Concurrently, the adjusting arm also undergoes passive adjustments, allowing both the longitudinal-swing-arm and the wheel assembly to conform to changes in terrain inclination. As illustrated in Figure 3, this adaptation facilitates alignment with the side slopes. Ensuring that each tire maintains proximity to a vertical orientation relative to the road surface while keeping the body level remains paramount.

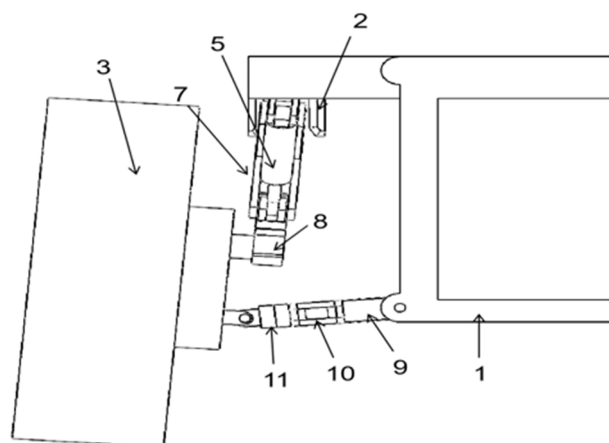


Figure 3. Schematic diagram of the wheel adaptation of the new vertical- and horizontal-arm independent suspension to a single side slope: 1 is the body; 2 is the limit slot; 3 is the wheel part; 4 is the adjusting arm 1; 5 is the gas spring; 6 is the regulating arm 2; 7 is the upper arm; 8 is the lower arm; 9 is the front arm; 10 is the short rod; and 11 is the rear arm.

Obstacle-crossing leg lifting: When the current side encounters an obstacle of a certain height, the four hydro-pneumatic springs start to operate actively. Firstly, the four wheels are partially lifted through active elongation, that is, the entire longitudinal-swing-arm is elongated and upright, thereby lifting the entire body. Next, the hydro-pneumatic spring of either the left front wheel or the right front wheel continues to extend, while the others remain stationary. After the short rod rotates backward to a certain angle in the forward direction of the body, the hydro-pneumatic spring begins to contract actively, and the short rod continues to rotate backward until the transverse arm is in the horizontal position. It then starts to turn back, and at this point, the wheel part is gradually lifted. When it is raised to the highest point, the hydro-pneumatic spring continues to contract, causing the wheel part to move forward slowly, thereby achieving the function of lifting the leg and surmounting the obstacle. The movements of lifting the legs and putting them down are shown in Figures 4 and 5.

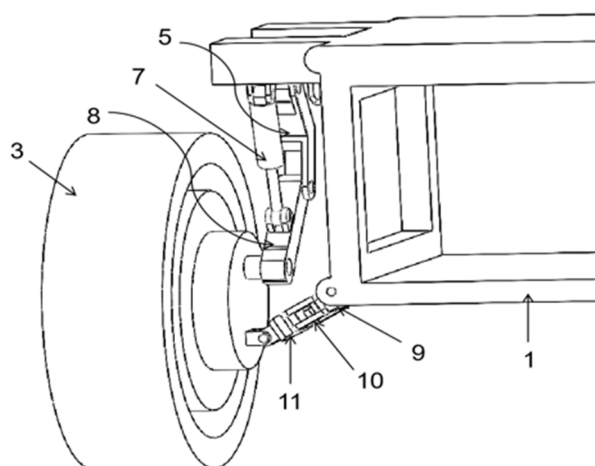


Figure 4. Schematic diagram of the wheel lifting in the new vertical- and horizontal-arm-type independent suspension: 1 is the body; 2 is the limit slot; 3 is the wheel part; 4 is the adjusting arm 1; 5 is the gas spring; 6 is the regulating arm 2; 7 is the upper arm; 8 is the lower arm; 9 is the front arm; 10 is the short rod; and 11 is the rear arm.

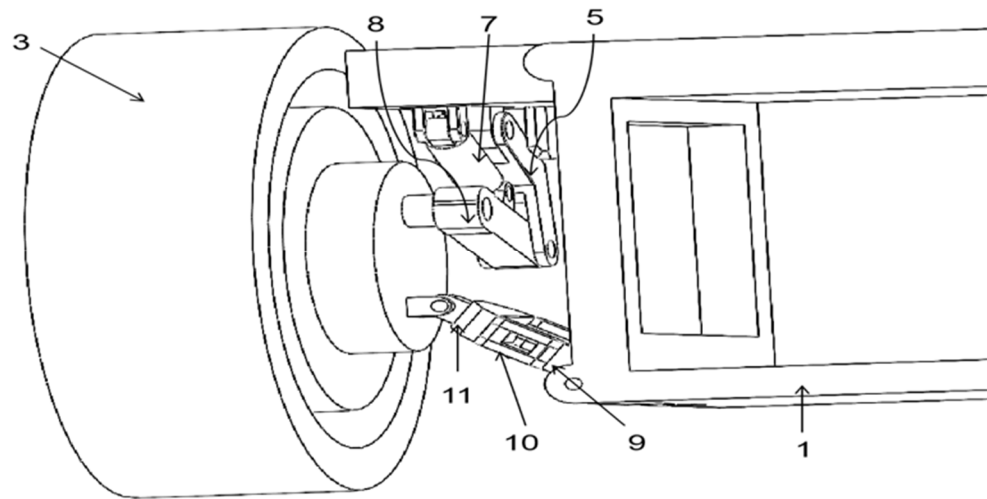


Figure 5. Schematic diagram of the new vertical- and horizontal-arm independent suspension: 1 is the body; 2 is the limit slot; 3 is the wheel part; 4 is the adjusting arm; 5 is the gas spring; 6 is the regulating arm; 7 is the upper arm; 8 is the lower arm; 9 is the front arm; 10 is the short rod; and 11 is the rear arm.

At the same time, due to the presence of the limit groove, the upper longitudinal arm gradually returns to normal when the mechanism moves backward to lift the leg. Thus, the entire wheel part is restored to its normal state. To ensure that the tire part is not overly skewed, the rotation angle of the longitudinal arm should not be adjusted excessively. This guarantees that the unmanned ground platform has a certain passing capacity. The vertical road surface of the wheel part can maintain the grip force of the wheel part as much as possible without a significant reduction, thereby enabling efficient driving ability and enhancing the ground-passing ability of the unmanned ground platform. Moreover, since the mechanism only makes the wheel part perpendicular to the road surface while the body remains nearly horizontal, the overall stability and comfort of the vehicle are ensured.

The suspension design offers the following advantages:

1. The innovative independent suspension system, featuring both vertical and horizontal arms, is capable of adapting to a wide range of complex road surfaces. This design ensures that the overall height and flexibility of the suspension remain unaffected by the lateral adjustment mechanism of the horizontal arm. Additionally, through self-adjustment capabilities, this mechanism allows for optimal tire grip and enhanced obstacle-surmounting performance.

2. At its core, the structure comprises a longitudinal-swing-arm mechanism, in conjunction with a horizontal-arm mechanism. This configuration guarantees that movement related to lifting legs and overcoming obstacles remains unobstructed while effectively accommodating lateral slopes or obstacles encountered on intricate terrains such as large potholes or continuously uneven road sections. The adaptation to a lateral terrain or obstacles primarily relies on adjustments made via the horizontal-arm mechanism without compromising its ability to navigate other challenges.

3. Analysis of the Obstacle-Crossing Capability of Unmanned Ground Platforms

This section begins by examining the advantages of the current suspension mechanisms used in unmanned ground platforms regarding longitudinal-terrain adaptation, while also addressing their limitations in lateral-terrain adaptability. It includes terrain diagrams depicting both single typical obstacles and composite obstacles based on real-world scenarios. Subsequently, using the actual parameters of the PIX autopilot chassis, a de-

tailed discussion is presented on its capability to traverse steps and trenches. Calculations were performed to predict potential improvements in the maximum passing height and width achievable through the implementation of new longitudinal- and transverse-arm suspensions, thereby providing a theoretical foundation for enhancing both the terrain adaptability and obstacle-surmounting capabilities of unmanned ground platforms.

3.1. Terrain Analysis

A review of the existing literature concerning suspension mechanisms for unmanned ground platforms—both domestically and internationally—reveals that while these mechanisms exhibit robust terrain adaptability and obstacle-crossing abilities in the longitudinal plane, they demonstrate significant deficiencies in the case of lateral plane performance (e.g., unilateral slopes, round pits, or large pit sections). For instance, Yang [20] identified various types of unstructured obstacles commonly encountered in practice; beyond ladder-like barriers and slope challenges, uneven-height roads flanking either side were highlighted as critical terrains. Additionally, compound obstacles including those involving trenches were categorized under single-type obstructions within this context.

Currently, most suspension systems are primarily designed to adapt to the terrain in the forward direction of the vehicle; however, they lack sufficient adaptability for lateral slopes and obstacle sections. Additionally, some newer suspension designs are only suitable for small detection vehicles or are based on simplified models that fail to account for the complex terrain environments encountered by unmanned ground platforms in comparison to manned vehicles.

In reality, unstructured environments, such as mountainous and hilly areas, present complexities that exceed those depicted in typical obstacle terrains shown in diagrams. This paper categorized various types of obstacle terrains, as illustrated in Figure 6, which included both typical and composite obstacle terrains. Typical obstacle terrains consist of step obstacles, trenches, unequal heights on both sides, and lateral slopes, while composite obstacle terrains encompass polynomial curve terrains and comprehensive composite obstacles (which integrate characteristics of steps, lateral slopes, and trenches). The composite unequal-height lateral slope represents a combination of varying heights alongside lateral inclines on both sides; its primary purpose is to assess the adaptability of the vehicle to lateral-terrain conditions.

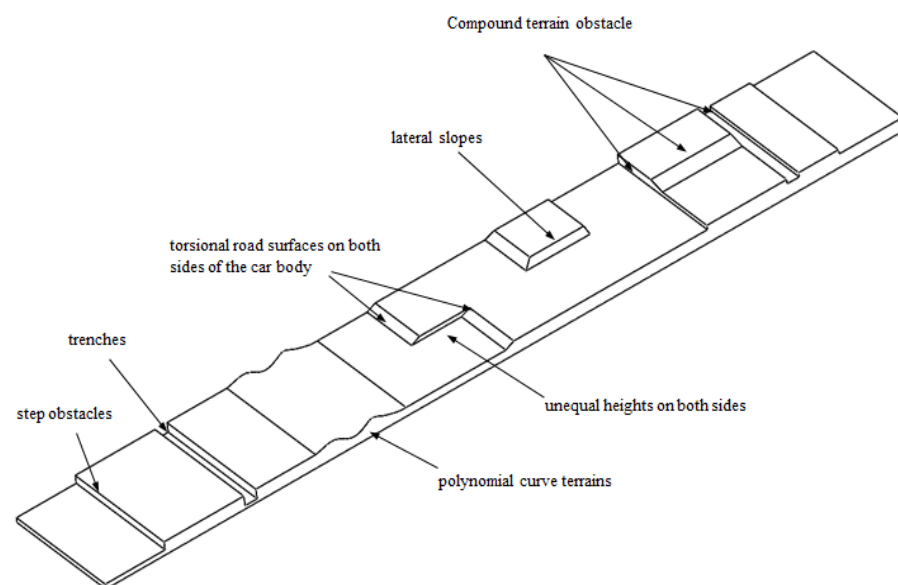


Figure 6. Comprehensive unstructured obstacle terrain.

3.2. Analysis of Step and Trench Negotiation Capabilities

The research presented in this paper was founded on the model construction and simulation of an actual vehicle with the PIX autonomous driving chassis. Hence, the aforementioned mechanical model analysis was calculated based on real vehicle parameters, and the ratio of the obstacle height/width to the vehicle radius could be obtained. The height and width of obstacle crossing are significant indicators for measuring the obstacle-crossing ability of vehicles. A higher obstacle-crossing height and a wider obstacle-crossing width imply that the vehicle can adapt to a greater variety of complex terrains and enhance its passing capacity in an unstructured environment. The variation in the wheel contact force reflects the interaction between the wheel and the ground.

The parameters of the PIX autonomous driving chassis are listed in Table 1, and the ratio can be derived from the calculation formula for the steps as stipulated in “automotive theory” [23]. Thus, it can be concluded that the rear-wheel obstacle negotiation height of a four-wheel-drive vehicle is approximately 174 mm.

Table 1. Real vehicle parameters with the PIX autonomous driving chassis.

Real Car Parameters	Value
Drive way	4 × 4
Size (mm)	2490 × 1550 × 590
Attachment coefficient φ	0.72
Wheel radius, R (mm)	300
Deadweight, m (kg)	200
Maximum load, G (kg)	1200
Wheel base, L (mm)	1900

The total travel of the active suspension is approximately 190 mm; therefore, the expected negotiable step height is 364 mm. In practice, by shifting the center of gravity rearward, the obstacle negotiation capability of the front wheel can fully exceed this height. However, due to the limitations imposed by the rear wheel’s obstacle negotiation capability, the overall obstacle negotiation capability is restricted.

Similarly, the maximum trench-crossing width for this general four-wheel-drive vehicle can be calculated to be approximately 545 mm. With the use of a new type of longitudinal- and transverse-arm suspension, the active adjustment of the suspension enables a positional difference of about 50 mm in the longitudinal direction between the left and right wheels. Therefore, it is anticipated that the maximum width that the unmanned ground platform can traverse through a trench is approximately 595 mm.

4. Simulation of the Autonomous Obstacle-Crossing Capability of Unmanned Ground Platforms

In this paper, the solid model of a vertical- and horizontal-arm unmanned ground platform was established in the ADAMS simulation platform, and the different key obstacle-surmounting actions of the platform in the face of different obstacles were planned to show its autonomous obstacle-surmounting capability. Using the ADAMS and MATLAB/Simulink joint simulation, the specific experimental process and data were obtained. Next, according to the aforementioned theoretical analysis, the vertical- and horizontal-arm unmanned ground platform’s obstacle-surmounting and obstacle-crossing ability, through slopes and compound typical obstacles, was determined and verified.

4.1. Construction of a Virtual Prototype

Firstly, the Solidworks model of an unmanned ground platform with a new vertical- and horizontal-arm independent suspension was established in Solidworks, as shown in Figure 7. Next, the model was imported from Solidworks into ADAMS, and the model in the ADAMS simulation platform is shown in Figure 8. At the same time, the terrain obstacle model shown in Figure 6 was imported as the obstacle road surface, and relevant constraints, contact forces, and driving forces were added.

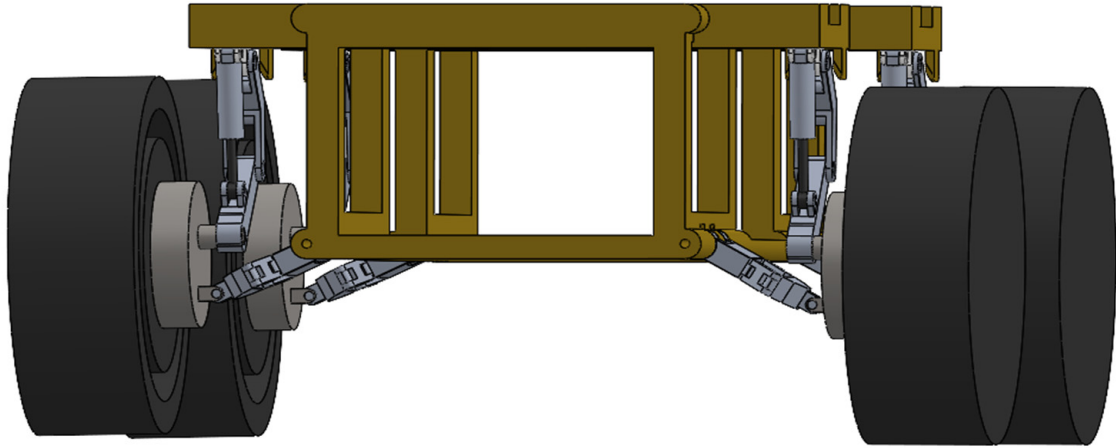


Figure 7. Solidworks model of the unmanned ground platform with a new type of transverse- and longitudinal-arm independent suspension.

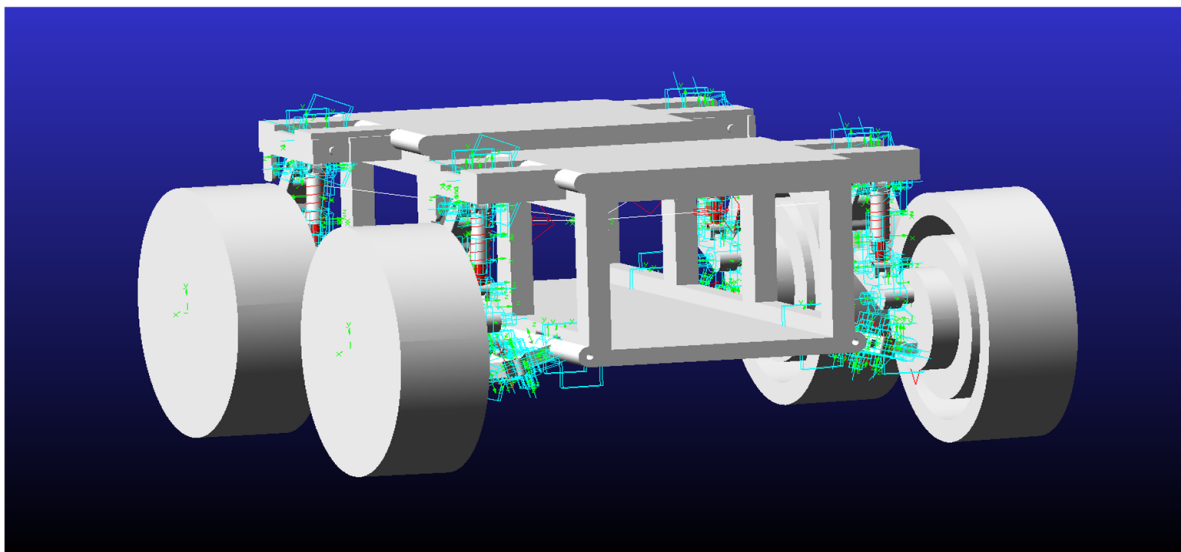


Figure 8. ADAMS model of the new type of transverse- and longitudinal-arm independent suspension.

Through the system design of ADAMS, a control module was generated in MATLAB/Simulink, as shown in Figure 9, where the left side was the input signal, and the right side was the output signal, which controlled the four wheels of the unmanned ground platform and the drive of the hydro-pneumatic spring, respectively. By setting the corresponding input value, the obstacle-crossing action planning of the simulation motion was controlled.

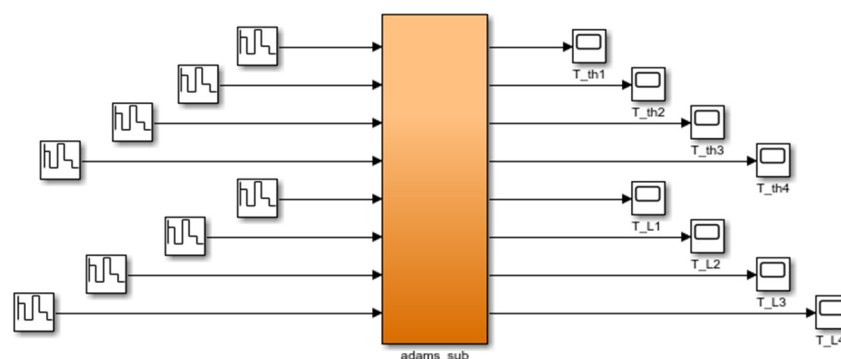


Figure 9. MATLAB/Simulink control module of the new type of transverse- and longitudinal-arm independent suspension.

4.2. Key Action Planning for Obstacle Crossing

When an unmanned ground platform encounters obstacles, it is necessary to cross the obstacles autonomously according to the obstacle form. Therefore, the unmanned ground platform and the terrain obstacle model were built, and the unmanned ground platform needed to plan the obstacle-crossing key actions and postures was based on the aforementioned unmanned ground platform model. After the obstacle-crossing planning was completed, the ADAMS virtual prototype technology was used to simulate and analyze the key planning actions of the platform with the new vertical- and horizontal-arm suspension to determine whether each obstacle was successfully crossed, and MATLAB R2021b software was used to obtain detailed and abundant data. The new vertical- and horizontal-arm independent suspension model and the obstacle terrain shown in Figure 8 were imported into ADAMS View 2020 software to carry out the obstacle-crossing simulation analysis of the unmanned ground platform. The obstacle-crossing process of each obstacle is shown in Figures 10–12. According to the experiments conducted, the structure design passed smoothly, and the specific results are as follows.

Figure 10 illustrates the entire process of the unmanned ground platform crossing a vertical obstacle. In Step 1, the active suspension of the rear wheels of the platform contracted, causing a slight rearward shift in its center of gravity. In Step 2, the speed and driving force of the left wheel decreased, while those of the right wheel remained unchanged or increased; simultaneously, the active suspension of the right front wheel began to contract until the right front wheel was lifted above the step. In Step 3, the speed and driving force of the right wheel decreased, while those of the left wheel remained unchanged or increased; concurrently, the active suspension of the left front wheel began to contract until the left front wheel was lifted above the step. In Step 4, the speed and driving force of the left wheel decreased, while those of the right wheel remained unchanged or increased; at the same time, the active suspension of the right rear wheel began to contract until the right rear wheel was lifted above the step. In Step 5, the speed and driving force of the right wheel decreased, while those of the left wheel remained unchanged or increased; simultaneously, the active suspension of the left rear wheel began to contract until the left rear wheel was lifted above the step. In Step 6, the unmanned ground platform returned to its initial state.

Step 1 was the preparation phase, Steps 2 to 5 were the obstacle-crossing phase, and Step 6 marked the end of the crossing phase. This outlines the process of the unmanned ground platform overcoming a step obstacle.

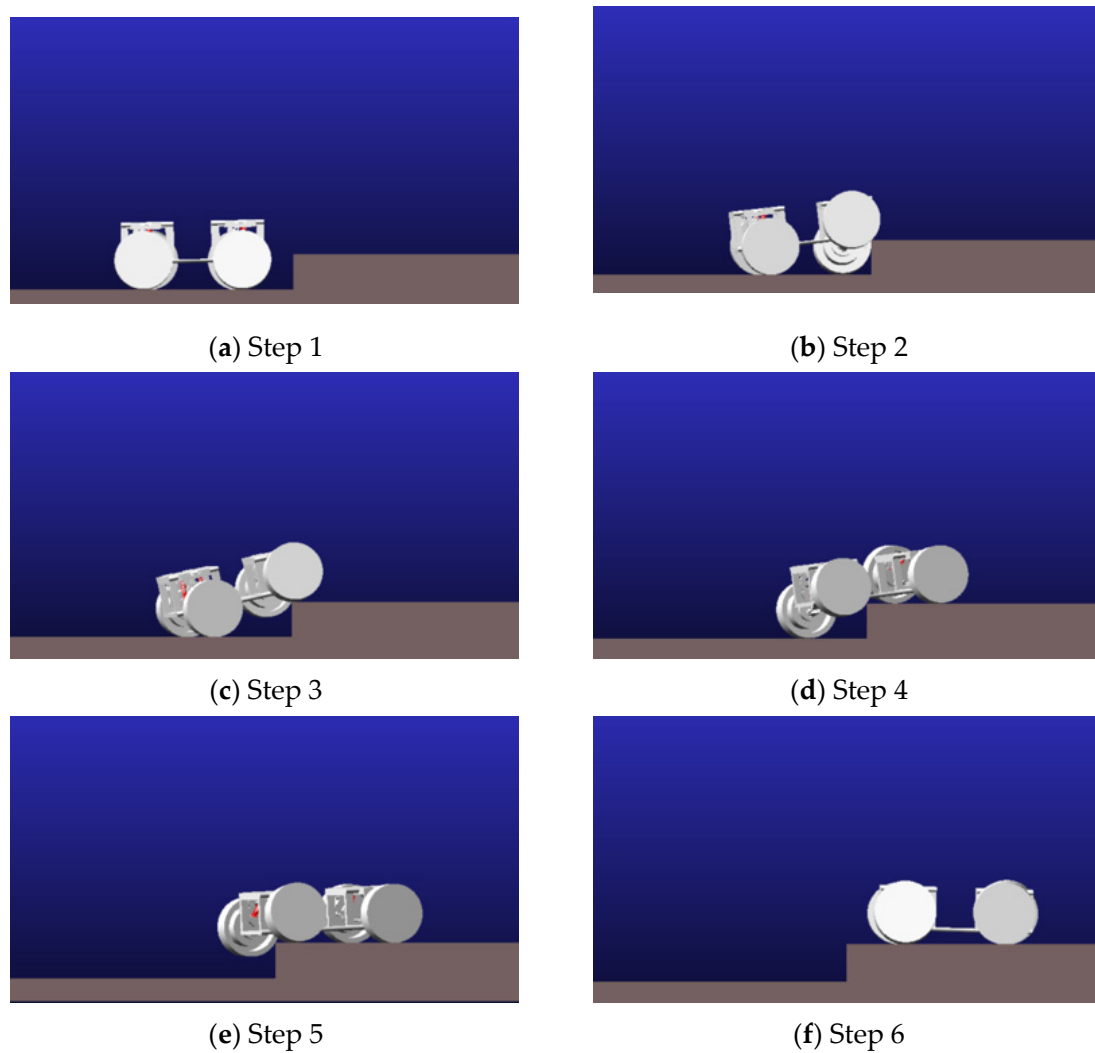


Figure 10. Process of overcoming vertical obstacles.

Figure 11 illustrates the entire process of the unmanned ground platform crossing a trench. In Step 1, the unmanned ground platform extended its active suspension to a certain height. In Step 2, the active suspension contracted, causing a positional difference between the left and right wheels (i.e., as shown in Figure 11b, the left front wheel was in the front, and the right front wheel was behind). In Step 3, after the suspension was adjusted, the unmanned ground platform accelerated forward. In Step 4, the left front wheel of the unmanned ground platform first touched the opposite side of the trench, causing the front of the vehicle to be lifted slightly due to the impact between the wheel and the trench, while the driving force of the rear wheels increased, allowing the left front wheel to cross the trench. In Step 5, after the left front wheel crossed the trench, the right front wheel was able to cross the trench and reach the opposite side. Steps 6 and 7 followed the same crossing method as the aforementioned front wheels. In Step 8, the unmanned ground platform returned to its initial state.

Steps 1 and 2 were the preparation stage, Steps 3 to 7 were the crossing stage, and Step 8 was the end of the crossing stage. This is the process of the unmanned ground platform crossing a trench.

Figure 12 illustrates the process of the unmanned ground platform crossing a composite obstacle surface. In Step 1, the center of gravity of the unmanned ground platform shifted backward, the speed and driving force of the left wheel decreased, and the speed and driving force of the right wheel remained unchanged or increased; simultaneously,

the active suspension of the right front wheel began to contract until the right front wheel was lifted above the composite step. In Step 2, similarly, the right front wheel lifted and crossed onto the composite step, and the crossing action of the rear wheels was planned accordingly. In Step 3, when the unmanned ground platform crossed the composite step, due to the characteristics of the suspension, the entire vehicle passively adapted to the slope on the side, thereby increasing the contact between the wheels and the ground and enhancing the vehicle's driving force. Steps 4, 5, and 6 had key crossing actions consistent with those in Figure 11 for crossing a trench. In Step 7, the unmanned ground platform returned to its initial state.

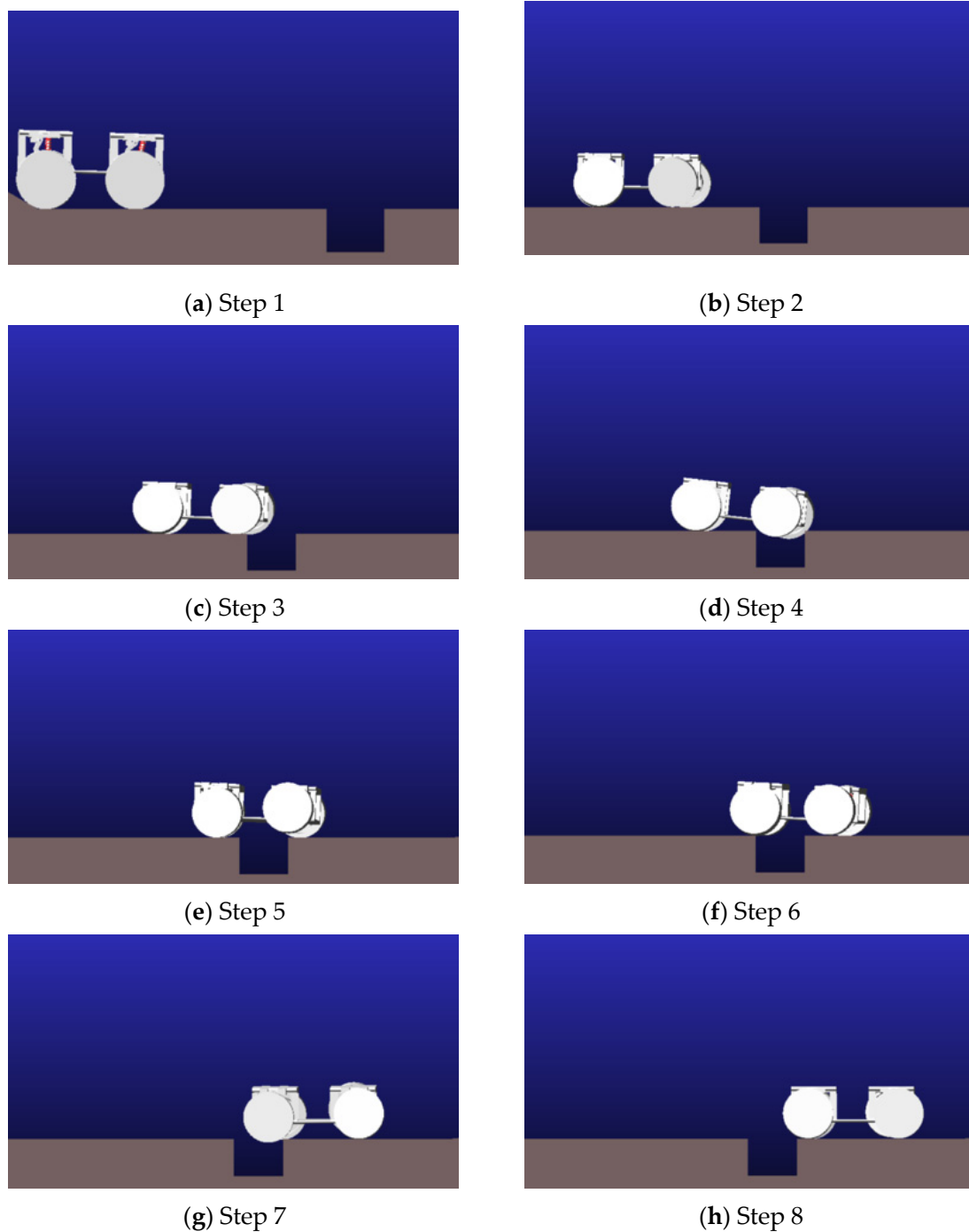


Figure 11. The process of crossing a trench.

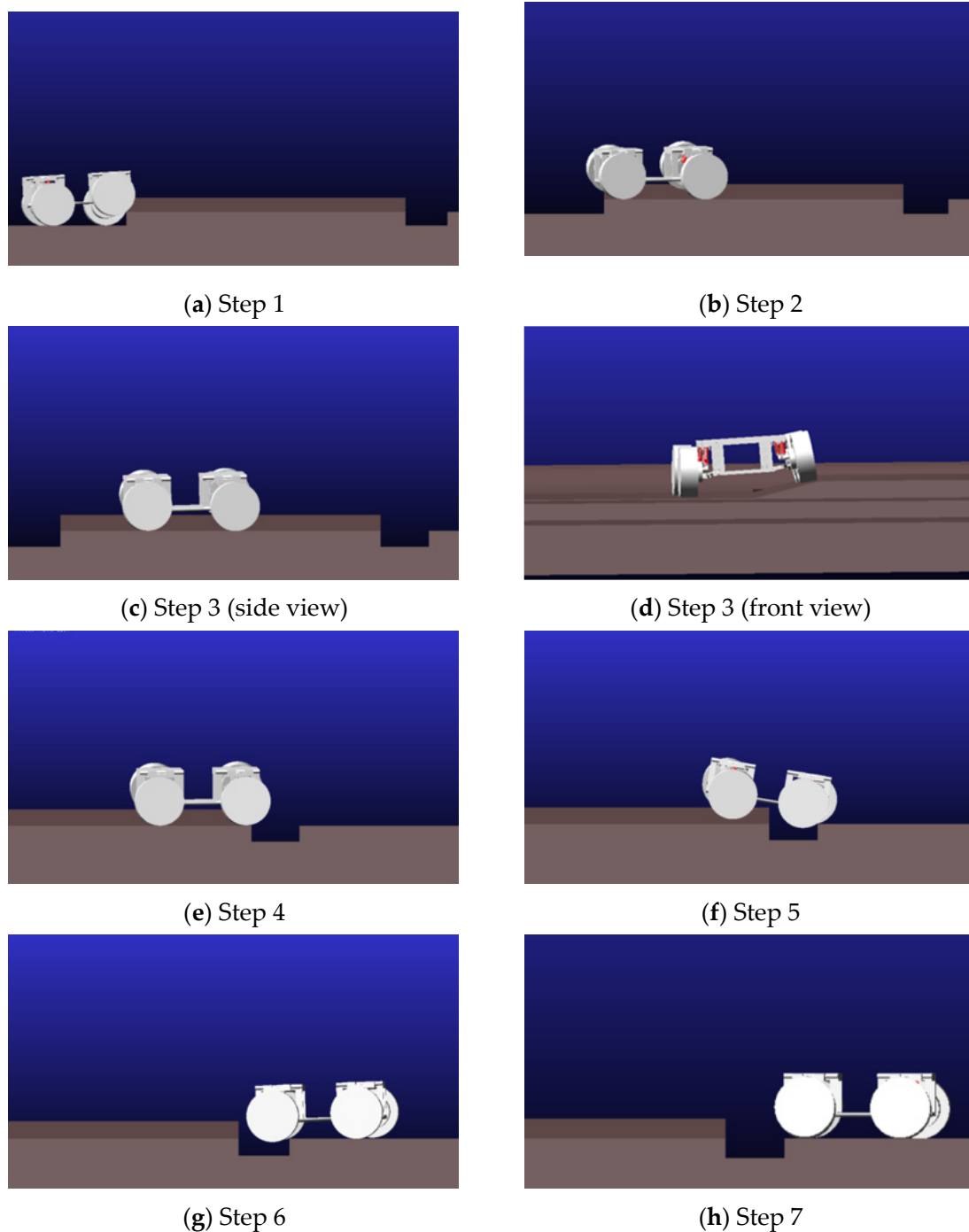


Figure 12. The process of crossing a composite obstacle.

Steps 1 and 2 were the initial stage of crossing the composite obstacle's step, Step 3 was the stage of passive adaptation on the composite step, Steps 4 to 6 were the stage of crossing the trench obstacle within the composite obstacle, and Step 7 was the concluding stage. This is the entire crossing process of the unmanned ground platform over a composite obstacle.

4.3. Results and Analysis

The evaluation of the crossing stability of an unmanned ground platform primarily refers to changes in the state parameters (including displacement, velocity, and acceleration) of its center of gravity in the vertical direction, while the evaluation of the side slope primarily refers to the comparison of the angle changes in the wheels on flat ground and

the side slopes. In this study, through ADAMS simulation, the displacement, velocity, and acceleration curves of the center of gravity of an unmanned ground platform during the crossing process as well as the angle change curves of the wheels were obtained, as shown in Figures 13–15.

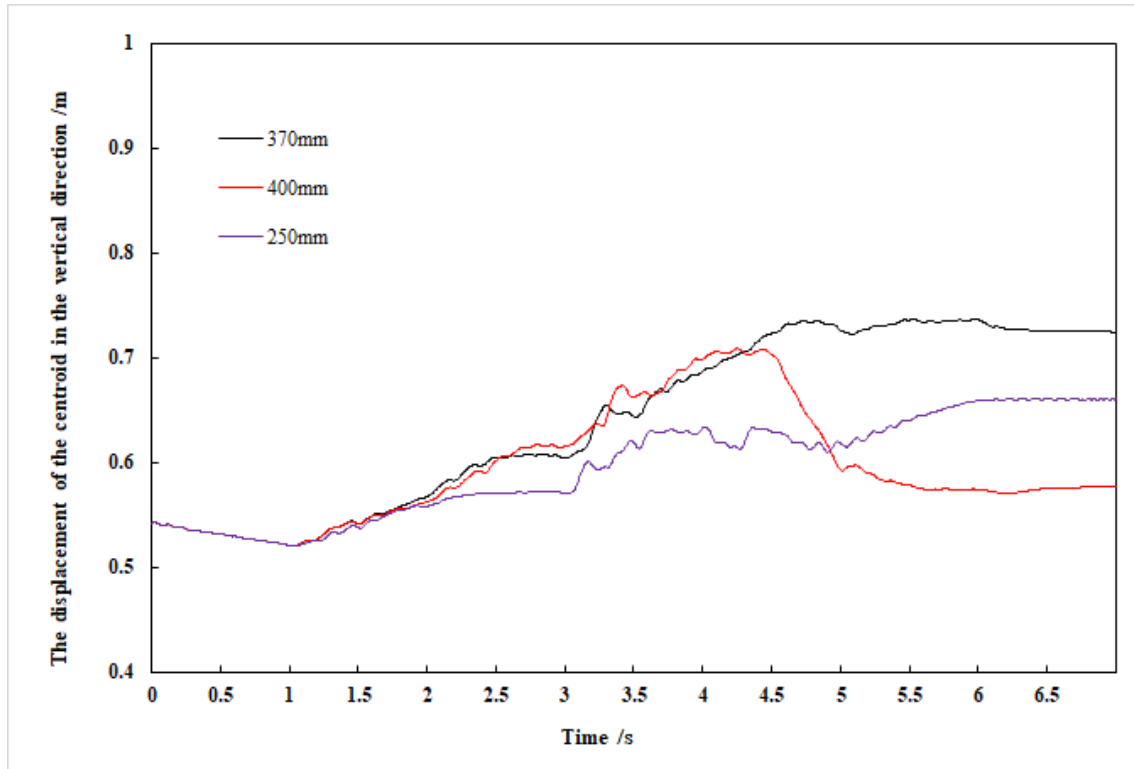


Figure 13. Simulation results of the more vertical obstacle-crossing capability of the unmanned ground platform.

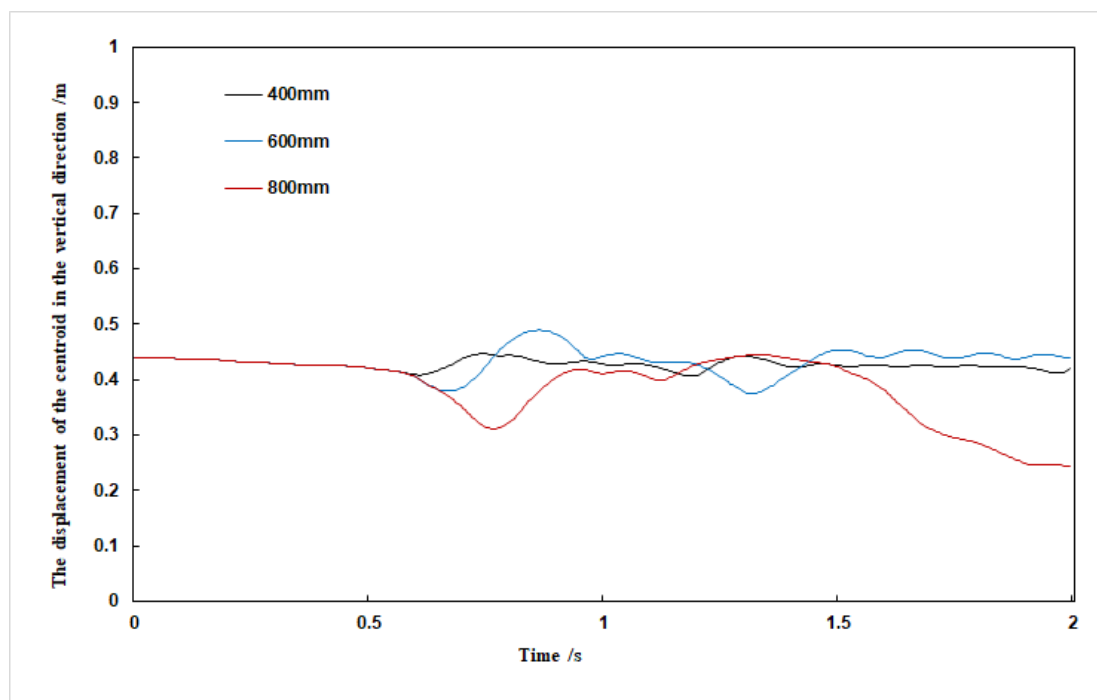
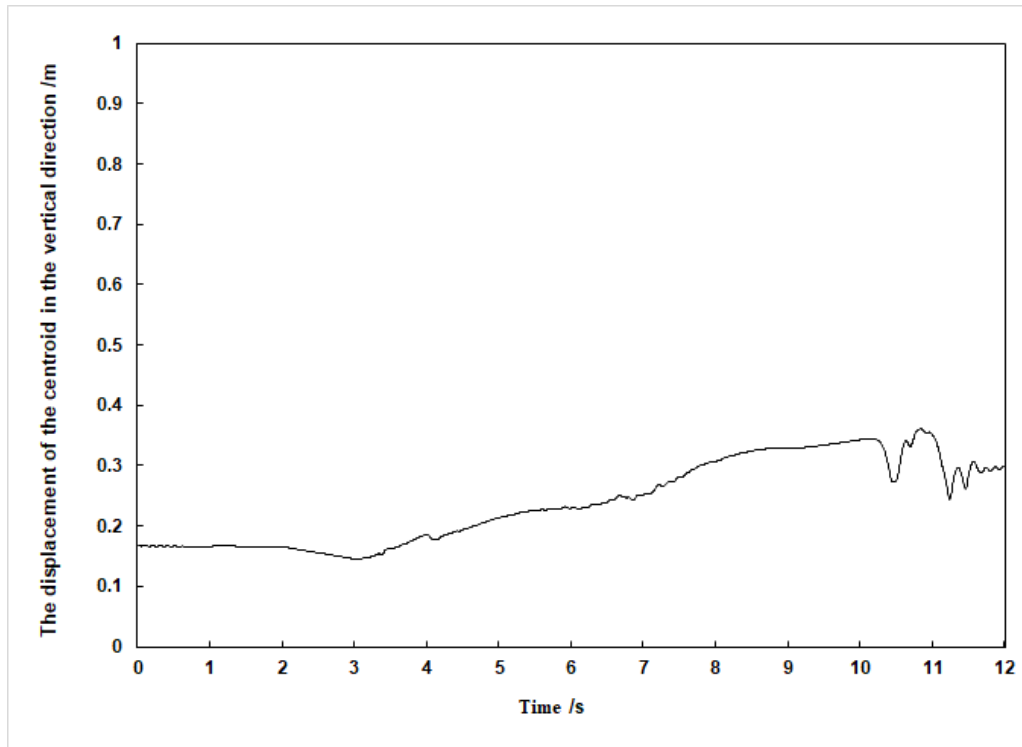
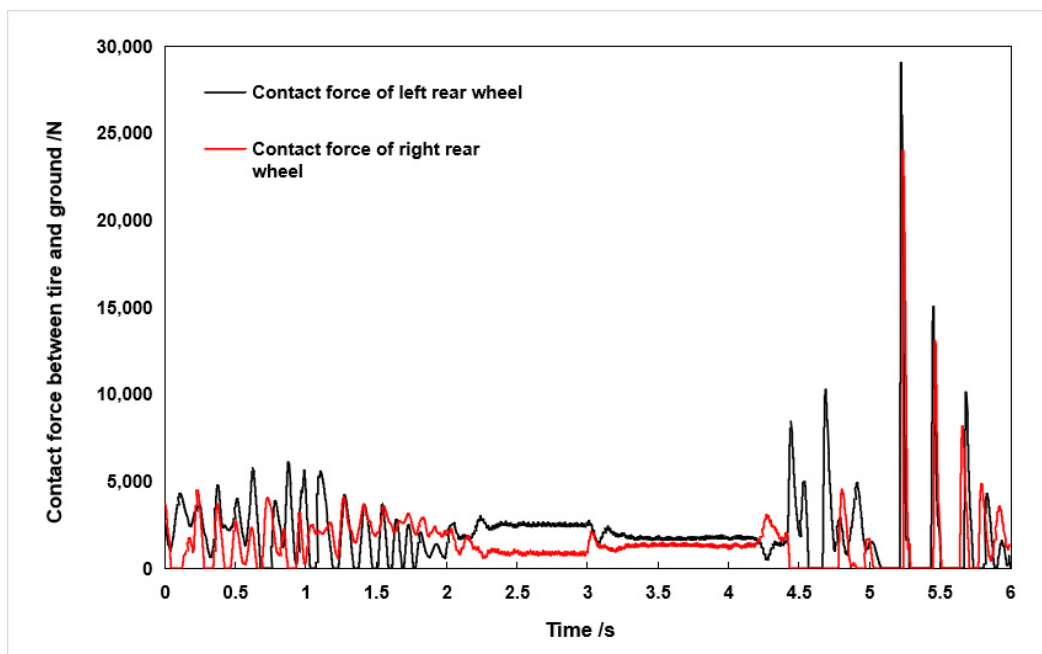


Figure 14. Simulation results of the trench-crossing capability of the unmanned ground platform.



(a) Shift change in the centroids in the vertical direction



(b) Change in the contact force between the tire and the ground

Figure 15. Comparison of the simulation results of the complex ability of an unmanned ground platform.

Figure 13 illustrates the curve variation in an unmanned ground platform (UGV) overcoming vertical obstacles of different heights. When traversing vertical steps of 250 mm and 370 mm height (see Figure 10), the UGV demonstrated good adaptability. However, for a step height of 400 mm, while the front wheels were able to clear the obstacle, the rear wheels showed a significant lack of obstacle-clearing capability, resulting in failure to cross the obstacle. The simulation results indicated that during the 0 to 1 s phase, the center-

of-mass displacement decreased due to the contraction of the rear wheel's oil-gas spring, causing the center of gravity to shift backward in preparation for overcoming the obstacle. From 1 to 3 s, the UGV successfully completed the obstacle-clearing action with the front wheels, which had lifted onto the step. The period from 3 to 6 s corresponded to the rear wheels attempting to clear the obstacle, where it can be observed that the rear wheels failed to clear the 400 mm high step but successfully cleared steps lower than 370 mm. Throughout the obstacle-clearing process, the center-of-mass displacement remained relatively stable, with the center-of-mass height increasing from 540 mm to 730 mm. The curve in the figure also indicates a brief fluctuation during the obstacle-clearing process, but overall, it maintained good stability.

Figure 14 depicts the curve variation in the UGV crossing ditches of different widths. When faced with a wider ditch (see Figure 11), the UGV adjusted its posture to achieve a staggered position of the front and rear wheels, thereby successfully crossing the obstacle. During the 0.5 to 1 s period, the front wheels traversed ditches measuring 400 mm, 600 mm, and 800 mm in width, respectively. However, during the 1 to 2 s period, the rear wheels were unable to pass through the 800 mm wide ditch; thus, the UGV could only cross ditches narrower than 600 mm. Despite significant impact effects during the obstacle-clearing process, with a notable change in the center-of-mass displacement and the maximum center-of-mass change distance being 110 mm, the UGV was able to complete the obstacle-clearing action smoothly, and the initial and final heights of the center of mass were essentially consistent, indicating good recovery capability.

Figure 15 compares the results of the UGV on a composite obstacle surface, where Figure 15a shows the change in the center-of-mass position of the UGV, and Figure 15b illustrates the variation in contact forces between the left and right rear wheels and the ground. The analysis method for the change in the center-of-mass position in Figure 15a is consistent with that in Figure 13. In Figure 15b, it can be seen that over time, the contact forces of both the left and right rear wheels were continuously changing. During the 0 to 2 s period, the rear wheels were engaged in crossing the steps of the composite obstacle. Starting from 2 s, the left rear wheel lifted onto a step with a slope. Beginning at 3 s, the contact forces of the left and right rear wheels gradually converged as during the 0 to 1 s period; when initially on the step, the vehicle's orientation needed to be adjusted to face the obstacle. From 3 to 4.25 s, the vehicle maintained a longitudinal driving state after adjusting its orientation, during which the contact forces of the left and right rear wheels continued to converge. The period from 4.25 to 6 s corresponded to the UGV transitioning from the slope of the composite obstacle to crossing the ditch. Therefore, the change in the center-of-mass position in Figure 15a and the contact force variation in Figure 15b during 2–4 s indicate that this structural design possesses good capability for traversing composite obstacles.

In summary, the simulation results demonstrate excellent performance of the novel independent suspension system with longitudinal and transverse arms in complex terrains, particularly in handling vertical obstacles, ditches, and slopes under special conditions.

5. Conclusions

We conducted an in-depth study on the autonomous obstacle-crossing capability of unmanned ground platforms in complex unstructured environments and proposed a novel longitudinal- and transverse-arm independent suspension system in this paper. This system aims to enhance the obstacle-crossing capability and terrain adaptability of unmanned ground platforms. Specifically, the newly proposed longitudinal- and transverse-arm independent suspension structure includes a longitudinal-swing-arm mechanism and a transverse-arm mechanism, which not only allow the tires to approach a vertical position relative to the ground when encountering obstacles to maintain good traction, but also

ensures that the vehicle body remains close to a horizontal state, thereby improving the overall stability and comfort of the unmanned ground platform.

Through the joint simulation verification of ADAMS and MATLAB/Simulink, the results indicate that the novel suspension system performed excellently in various typical obstacles (such as vertical steps and ditches) as well as in compound obstacle environments. The novel longitudinal- and transverse-arm independent suspension system demonstrated significant effects in enhancing the obstacle-crossing capability and terrain adaptability of unmanned ground platforms:

1. Step obstacles: The unmanned ground platform exhibited good adaptability when crossing steps of varying heights. For steps of 250 mm and 370 mm in height, the platform could successfully complete obstacle crossing; however, when the obstacle height increased to 400 mm, although the front wheels could successfully cross, the rear wheels failed to do so due to insufficient obstacle-crossing capability. Throughout the obstacle-crossing process, the center-of-mass displacement remained relatively stable, increasing from 540 mm to 730 mm, showcasing the advantage of this suspension system in maintaining vehicle stability.

2. Ditch obstacles: When facing ditches of varying widths, the unmanned ground platform adjusted its posture to achieve a staggered position of the front and rear wheels, thereby successfully crossing smaller-width obstacles. The platform could successfully pass through ditches not exceeding 600 mm in width; however, when attempting to cross an 800 mm wide ditch, the rear wheels failed to cross, resulting in an overall obstacle-crossing failure. Despite the evident impact effects, with a maximum center-of-mass displacement of 110 mm, the platform still maintained good stability and demonstrated excellent recovery capability.

3. Compound obstacles: When confronted with compound obstacles that included vertical barriers, ditches, and slopes, the unmanned ground platform ensured optimal tire-ground contact by passively adapting to lateral terrain through its suspension and actively crossing obstacles, allowing the tires to approach a vertical position relative to the ground to maintain good traction, further proving the superior performance of this suspension system under complex terrain conditions.

In summary, the newly proposed longitudinal- and transverse-arm independent suspension system is of significant importance for improving the obstacle-crossing performance of unmanned ground platforms in complex unstructured environments such as mountainous areas, hills, and mining regions. The suspension system not only enhances the vehicle's adaptability to various obstacles, but also improves its maneuverability and safety under harsh conditions. Future work will focus on further optimizing the design details of the suspension structure and exploring more advanced materials and technological applications, with the aim of achieving higher obstacle-crossing efficiency and greater overall stability. With the development of unmanned driving technology, our research outcome is expected to provide more reliable support for unmanned ground platforms in the military operations and civilian emergency response fields.

Future work will focus on further optimizing the suspension structure parameters and the application of new materials to improve its adaptability and efficiency. Mikita, T. et al. [24] explored the modeling of vehicle mobility in forest environments, pointing out the limitations of current sensor technology in complex natural environments. This suggests that we need to pay more attention to the reliability and accuracy of sensor data and on how to integrate mechanical design to compensate for these deficiencies. In the future, by exploring intelligent control systems, we will enhance the multi-task processing capabilities, popularize modular design, expand the application range, improve system

performance, deepen theoretical research, and develop more advanced control algorithms to ensure the continuous innovation and wide application of this technology.

6. Patents

A Chinese invention patent has been applied for our new type of independent suspension structure with longitudinal and lateral arms (application number: 202410423465.1).

Author Contributions: Conceptualization, methodology, resources, writing-review and editing, supervision, project administration and funding acquisition, J.L.; Software, validation, formal analysis, data curation, writing-original draft preparation and visualization, Y.X.; Investigation, Y.H. All authors have read and agreed to the published version of the manuscript.

Funding: This research was granted financial support from the Innovation and Entrepreneurship Projects for College Students (grant number S202410580053) and the Special Talent Training Program (grant number zlgc2024018).

Data Availability Statement: The original contributions presented in the study are included in the article, and further inquiries can be directed to the corresponding author.

Conflicts of Interest: The authors declare no conflicts of interest.

References

- Shoemaker, C.M.; Bornstein, J.A. The Demo III UGV program: A testbed for autonomous navigation research. In Proceedings of the 1998 IEEE International Symposium on Intelligent Control (ISIC) Held Jointly with IEEE International Symposium on Computational Intelligence in Robotics and Automation (CIRA) Intell, Gaithersburg, MD, USA, 17 September 1998; IEEE: Piscataway, NJ, USA, 1998; pp. 644–651.
- Skultety, E. Terrain Characterization Methods of Unstructured Terrain for an Autonomous Mobile Robot. Master's Thesis, Oslomet-Storbyuniversitetet, Oslo, Norway, 2023.
- Nowakowski, M.; Janos, R.; Semjon, J.A.N.; Varga, J. Removal system for unmanned ground vehicles using a modular robotic arm. *MM Sci. J.* **2024**, *2024*, 7795–7799. [[CrossRef](#)]
- Li, R.U.S. Army "Mule"-Multi-functional General/Logistics Robot Vehicle. *Foreign Tanks* **2006**, *8*, 24–25.
- Chun, W.H.; Beck, M.S.; Stinchcomb, J.T.; Clemens, D.A.; Dunne, J.C.; Anderfaas, E.N. Articulated Vehicle Suspension System Shoulder Joint. U.S. Patent 7261176B2, 28 August 2007.
- He, J.; Ren, C.; Wu, K.; He, Q.; Zhao, Y.; Wang, Z. Analysis and Testing of Obstacle-Crossing Performance of an Eight-Wheeled Four-Suspension Unmanned Mobile Platform. *J. Agric. Mach.* **2019**, *50*, 367–373.
- Zhang, T.; Wang, T.; Wu, Y.; Zhao, Q. Design and Implementation of All-Terrain Unmanned Vehicles. *Robotics* **2013**, *35*, 657–664.
- Fang, Y. Analysis and Control System Design of Wheeled-Leg Hybrid Mobile Robots for Obstacle Crossing. Master's Thesis, Harbin Institute of Technology, Harbin, China, 2010.
- Liu, X.; Wu, W.; Jia, X.; Yao, X. Analysis of the Vertical Obstacle-Crossing Capability of a Six-Wheeled Vehicle. *J. Chongqing Jiaotong Univ. (Nat. Sci. Ed.)* **2019**, *38*, 128–133.
- Sreenivasan, S.V.; Waldron, K.J. Displacement Analysis of an Actively Articulated Wheeled Vehicle Configuration With Extensions to Motion Planning on Uneven Terrain. *ASME J. Mech. Des.* **1996**, *118*, 312–317. [[CrossRef](#)]
- Iagnemma, K.; Rzepniewski, A.; Dubowsky, S.; Schenker, P. Control of robotic vehicles with actively articulated suspensions in rough terrain. *Auton. Robot.* **2003**, *14*, 5–16. [[CrossRef](#)]
- Wang, F. Design and Performance Analysis of All-Terrain Wheeled Mobile Robots. Master's Thesis, Southwest Jiaotong University, Chengdu, China, 2018.
- Zhang, S. Design Simulation and Optimization of a Terrain-Adaptable Rescue Robot Mobile Platform. Master's Thesis, Tianjin University of Technology, Tianjin, China, 2019.
- Lindemann, R.; Voorhees, C. Mars Exploration Rover mobility assembly design, test and performance. In Proceedings of the 2005 IEEE International Conference on Systems, Man and Cybernetics, Waikoloa, HI, USA, 12 October 2005; IEEE: Piscataway, NJ, USA, 2005; Volume 1, pp. 450–455.
- Wettergreen, D.; Moreland, S.; Skonieczny, K.; Jonak, D.; Kohanbash, D.; Teza, J. Design and field experimentation of a prototype lunar prospector. *Int. J. Robot. Res.* **2010**, *29*, 1550–1564. [[CrossRef](#)]
- Wagner, M.D.; Apostolopoulos, D.; Shillcutt, K.; Shamah, B.; Simmons, R.; Whittaker, W. The science autonomy system of the nomad robot. In *Proceedings 2001 ICRA, Proceedings of the IEEE International Conference on Robotics and Automation (Cat. No. 01CH37164)*, Seoul, Republic of Korea, 21–26 May 2001; IEEE: Piscataway, NJ, USA, 2001; Volume 2, pp. 1742–1749.

17. Apostolopoulos, D. Analytical Configuration of Wheeled Robotic Locomotion. Ph.D. Thesis, Carnegie Mellon University, Pennsylvania, PA, USA, 2001.
18. Wei, Y.; Cheng, Z.; Jiang, H.; Zhang, J.; Li, Z. Design of a Six-Wheel Guided Rod Linked Suspension for Mobile Robots and Its Stability Analysis. *Robotics* **2013**, *35*, 665–671.
19. Li, S. Experimental Study on Design Parameters Optimization and Folding Span of Rocker Arm Suspension of Lunar Rover. Ph.D. Thesis, Harbin Institute of Technology, Harbin, China, 2010.
20. Yang, W. Design and Research of Adaptive Joint-Wheeled Mobile Robots. Master's Thesis, Southwest University of Science and Technology, Mianyang, China, 2020.
21. Tian, H.; Fang, Z.; Gu, Y. Dynamic Modeling and Influencing Factors Analysis of Wheel-Leg Robots for Obstacle Crossing. *Robotics* **2010**, *32*, 390–397.
22. Xu, Z.; Lu, J.; Yang, R.; Xiong, G.; Yang, H. Dynamic Stability Analysis and Control of Jointed Mobile Robots for Obstacle Crossing. *J. Beijing Inst. Technol.* **2005**, *25*, 311–314+336.
23. Yu, Z. *Automotive Theory*, 6th ed.; China Machine Press: Beijing, China, 2018; pp. 297–299.
24. Mikita, T.; Rybansky, M.; Krausková, D.; Dohnal, F.; Vystavěl, O.; Hollmannová, S. Mapping Forest Parameters to Model the Mobility of Terrain Vehicles. *Forests* **2024**, *15*, 1882. [[CrossRef](#)]

Disclaimer/Publisher's Note: The statements, opinions and data contained in all publications are solely those of the individual author(s) and contributor(s) and not of MDPI and/or the editor(s). MDPI and/or the editor(s) disclaim responsibility for any injury to people or property resulting from any ideas, methods, instructions or products referred to in the content.